JOURNAL OF MATERIALS SCIENCE 22 (1987) 1061–1066

Interfacial phenomena of plasma arc welding of mild steel and aluminium

T. ISHIDA
The Research Institute for Iron, Steel and Other Metals, Tohoku University, Sendai, Japan

The interfacial microstructures and intermetallic compounds produced by plasma arc butt fusion welding of aluminium to mild steel have been investigated. An intermetallic compound alloy layer formed at the interface region between mild steel and aluminium was determined using quantitative metallography and the mechanism of the intermetallic layer formation and growth was elucidated. The melt width and the alloy layer thickness decrease with increasing transfer-speed of the plasma torch. The intermetallic layers formed at the interface region between mild steel and aluminium are predominantly η-phase (Fe_2Al_5) and θ-phase ($FeAl_3$). The η-phase layer with columnar crystal grows rapidly as tongue-like structures in the direction of the mild steel substrate and the θ-phase layer with granular crystals projects slowly to the aluminium side in the course of solidification. As a result, many vacancies are produced in the η-phase layer. The structures of the melted zone and the fusion boundary of the mild steel change into grain refinement, whereas the melted zone of the aluminium has a eutectic structure of aluminium and θ-phase.

1. Introduction

The reaction between iron and aluminium is becoming increasingly important in many industrial processes such as the aluminium composites [1, 2], the friction welding of aluminium to iron [3], aluminium protective coatings [4, 5], the hot dipping and the cementation relevant to solid iron–liquid aluminium reactions [6–8], the diffusion welding [9–11] and the arc-welding of aluminium to iron [12, 13]. In the bonding of aluminium to iron, the formation of a layer of brittle intermediate phase occurs at the aluminium–iron interface. The intermetallic compound produced by the reaction of iron with aluminium can cause extreme embrittlement of the joint. The use of inserting metal, such as silver, nickel, copper and aluminium alloys [13–15] prevents the formation of this intermetallic compound. In the present experiment, the bonding of aluminium to iron has been carried out directly and rapidly in liquid phase without a filler metal, resulting in the formation of relatively thin intermediate layer at the interface region. The formation of such a thin layer may have hardly any influence on the strength of the joint.

The present investigation was initiated with the intention of metallurgically characterizing dissimilar-metal welding of the iron–aluminium system. This paper describes the interfacial microstructures and the intermetallic compounds produced by the fusion welding of mild steel and aluminium, with particular reference to the elucidation of the mechanism of the intermetallic compounds formation and growth at the Fe–Al interface.

2. Experimental procedure

The iron and aluminium materials used in this study were the commercial 5 mm thick mild steel and aluminium plates. The chemical compositions of these materials are given in Table I. These materials were cut to the dimensions of 50 mm × 100 mm and then the edges to be welded were ground and polished using an emery belt and paper, and were then cleaned.

The values of the fixed parameters on the welding condition are listed in Table II. I-typed butt welding without grooving of the pieces was done at a constant transfer-speed of the plasma torch using an argon plasma gas and Ar + H_2 or helium shielding gas. No filler metal was used. The butt bead welds were subsequently sectioned and polished perpendicular to the direction of weld plane. The prepared samples were examined by the Vickers microhardness test, optical microscopy and electron probe microanalysis (EPMA). The X-ray intensity profiles for the various elements across the welded region were established using the electron probe microanalyser operating at a

TABLE I Chemical compositions of mild steel and aluminium plates employed (wt %)

Specimen plate	Element									
	C	Ni	Cr	Si	Mn	P	S	Cu	Al	Fe
Mild steel (SS41)	0.13	0.020	0.043	0.16	0.58	0.024	0.021	–	0.027	99.0
Aluminium (A 1050)	–	–	–	0.20	0.05	–	–	0.05	99.5	0.20

0022–2461/87 $03.00 + .12

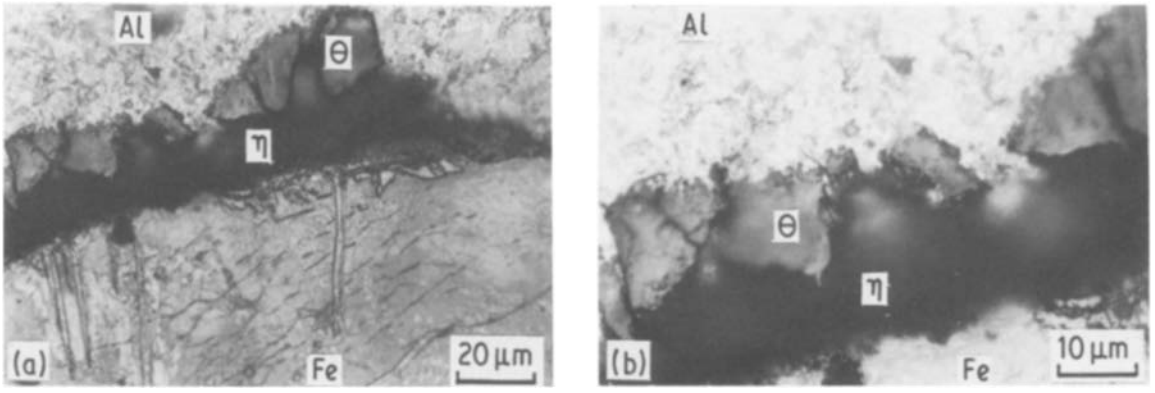

Figure 1 The solidifed microstructures of the interface between mild steel and aluminium produced by plasma arc fusion welding at an arc current of 130A on a transfer-speed of 2.75 mm sec^{-1}. Nital etch and 3% HF etch. (a) η and θ layers, and long slender tongue-like structures at the interfacial region. (b) The enlarged microstructure of the interface.

20 kV accelerating voltage with 0.01 μA beam current and employing LiF crystals for diffracting Fe$K\alpha$, ADP (ammonium dihydrogen phosphate) for diffracting Al$K\alpha$, and PbSD for diffracting $CK\alpha$ lines.

3. Results

The typical welding conditions of mild steel and aluminium under the plasma arc and the measured results of the mean melt width in the bead weld and the mean alloy layer thickness at the interface region are given in Table III. It is clear that the melt width and the thickness of the intermetallic compound alloy layer decrease with increased transfer-speed of the plasma torch.

Fig. 1 shows the solidified microstructures of the mild steel–aluminium interface region produced by plasma arc fusion welding at a transfer-speed of 2.75 mm sec^{-1}, using an argon plasma gas with a flow rate of 3.2 $dm^3 min^{-1}$ and a helium shielding gas with a flow rate of 14.5 $dm^3 min^{-1}$. Furthermore, the electron microprobe profile across the interface region is presented in Fig. 2. The profile indicates that the intensity ratio of Fe$K\alpha$ obtained by the EPMA trace is 44.2 and 31.6% in the η and θ parts of Fig. 2, respectively. The comparison with the intensity of known composition of various compounds is required in order to find the composition in the alloy layer from the observed intensity of the Fe$K\alpha$ and Al$K\alpha$. A conversion to the iron concentrations in the two parts of Fig. 2, assuming that the steel substrate is 100% iron, shows that the η and θ parts contain approximately 48.0 and 36.0 wt % iron, respectively. When these concentrations are compared with the concentration of iron in iron–aluminum intermetallic compounds, it appears that the η part corresponds to the η-phase Fe_2Al_5 (43.8 to 48.0 wt % [16, 17]) and the θ part the θ-phase $FeAl_3$ (38.4 to 42.7 wt % iron [16, 17]). This result is almost consistent with the view of the intermetallic layer formation of aluminium coating on aluminiumized steel [16]. In Fig. 1a, the η-phase (Fe_2Al_5) and θ-phase ($FeAl_3$) layers were detected in the interfacial region between mild steel and aluminium, where sharp tongue-like crystals stretched abruptly into the mild steel substrate from the root of η-phase layer and granular crystals projected into the aluminium from the θ-phase layer, as seen in Fig. 1b.

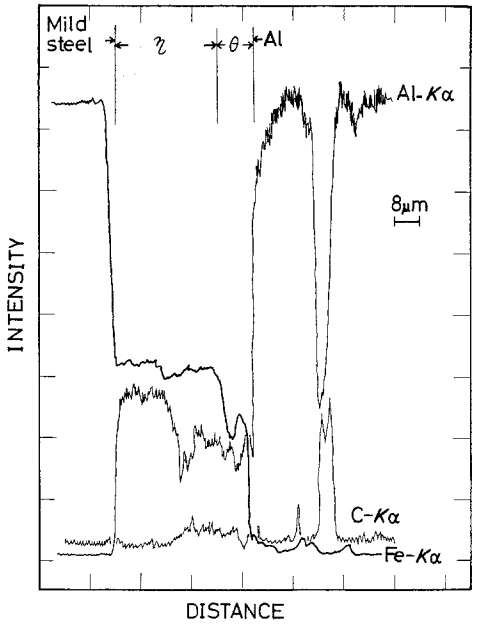

Figure 2 EPMA Traces of Fe$K\alpha$, Al$K\alpha$ and $CK\alpha$ rays across the interface between mild steel and aluminium at an arc current of 130 A on a transfer-speed of 2.75 mm sec^{-1}.

Fig. 3 shows the solidified microstructure of the mild steel–aluminium interfacial region at a transfer-speed of 4.67 mm sec^{-1}, using an argon plasma gas with a flow rate of 2.5 $dm^3 min^{-1}$ and an Ar + 10% H_2 shielding gas with a flow rate of 10.0 $dm^3 min^{-1}$. The result of the EPMA traces across the interfacial region is shown in Fig. 4. Optical microscopy and

TABLE II Welding conditions of mild steel to aluminium by plasma arc

Parameter	Values
Plasma arc type	Transferred type
Polality	Direct current straight polality
Electrode	Tungsten 6.0 ϕ mm
Nozzle diameter	3.0 ϕ mm
Plasma gas	Argon
Shielding gas	Ar + 10%H_2, He
Arc current	100, 115, 130A
Travel speed	2.75, 3.33, 4.67 mm sec^{-1}
Joint method	Single-pass butt welds without filler metal

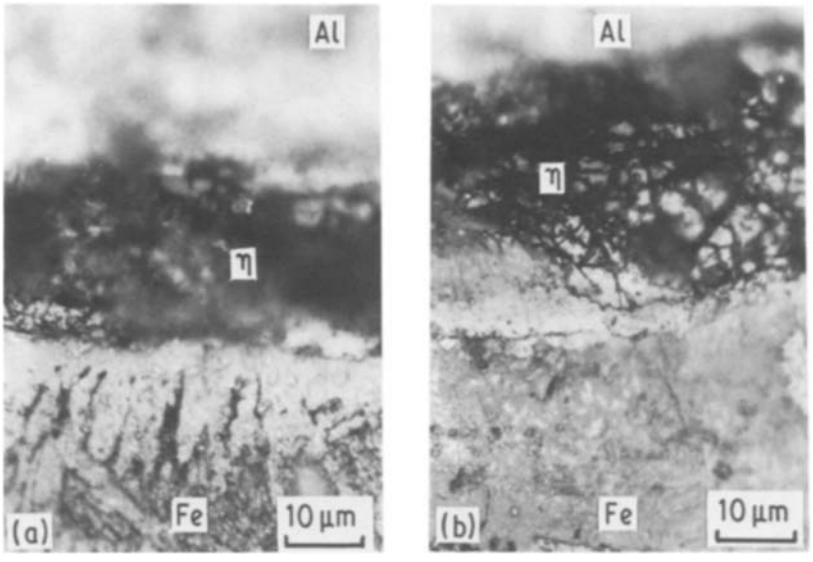

Figure 3 The microstructures of the interfacial region between mild steel and aluminium produced by plasma arc fusion welding at an arc current of 130A on a transfer-speed of 4.67 mm sec^{-1}. Nital etch and 3%HF etch. (a) η layer and tongue-like structures appearing at the interface. (b) The heterogeneous η layer containing a porous structure.

EPMA revealed that the η-phase layer and uneven protuberant tongue-like structure were formed at the interface region (Fig. 3a), and the η layer was relatively porous and θ layer was undetectable in this part (Fig. 3b).

Fig. 5 shows the microstructures of the melted zones of mild steel and aluminium, and the interfacial region of the mild steel between the melted and unmelted zones. It is apparent that the structure of the melted zone of mild steel changes into grain refinement (Fig. 5a), while the melted zone of aluminium has an eutectic structure of aluminium and θ-phase (Fig. 5b). Both minute pearlite–ferrite (Fig. 5c) and minute acicular pearlite–ferrite (Fig. 5d) interfaces can be detected metallographically in the fusion boundary region of the mild steel.

Fig. 6 shows the results of the microhardness tests across the interfacial region between mild steel and aluminium. The Vickers microhardness was measured with a loading of 50 g under a metallurgical microscope. The hardness became high in the intermetallic alloy layer formed at the interfacial region and low in the Al-melted zone. According to the more detailed study of Nishida *et al.* [18], the hardness of the η-phase (Fe_2Al_5) is *VHN* 870 to 1020, that of $\eta + \theta$-phase ($FeAl_3$) is *VHN* 670 to 870 and that of θ-phase is *VHN* 670 to 780. The hardness of the alloy layer obtained in this experiment may correspond to that of ($\eta + \theta$) phase. This suggests the formation of η- and θ-phase layers at the interfacial region.

4. Discussion

In the case of fusion joining of aluminium to mild steel, it was found that the intermetallic layers formed at the interface are predominantly η-phase (Fe_2Al_5) and θ-phase ($FeAl_3$). This phenomenon is analogous to the behaviour of the intermetallic compound layer formation at the interface between solid iron and molten aluminium [6, 19–22]. The so-called tongue-like structure which is formed on the interface between solid iron and molten aluminium is also produced in the case of the joining in liquid phase in the present study. This suggests that the tongue-like structure forms and grows during solidification. The mechanism of the formation and growth of intermetallic compound alloy layer in this interface may be considered in the following way, with reference to Fig. 7:

Namely, when the mild steel plate contacts the aluminium plate in liquid state beneath the plasma arc (Fig. 7a), mutual diffusion of the molten iron and the molten aluminium occurs at the area of contact and each metal is alloyed at the contact area (Fig. 7b). At that time, though the mutual solute concentrations at the contact-interface become relatively high, the concentrations in the bulk liquid are considered to be not so high as expected, due to the short-reaction time. After the plasma arc heat source passes, the melt-zone is allowed to be rapidly cooled and then to be in the course of rapid solidification. The formation of the intermetallic compound $FeAl_3$ having the lowest iron concentration, as seen in the Al–Fe phase diagram

TABLE III Typical examples of the fusion joining of aluminium to mild steel by the plasma arc

Welding conditions				Observed beads	
Current (A)	Travel speed (mm sec^{-1})	Plasma gas (dm^3 min^{-1})	Shielding gas (dm^3 min^{-1})	Melt width W_m (mm)	Alloy layer thickness W_A (μm)
130	2.75	Ar: 3.2	Ar + 10%H_2: 14.0	13.4	40
130	2.75	Ar: 3.2	He: 14.5	16.1	28
130	4.67	Ar: 2.5	Ar + 10%H_2: 10.0	10.0	25
130	4.67	Ar: 2.5	Ar + 10%H_2: 10.0	10.4	20

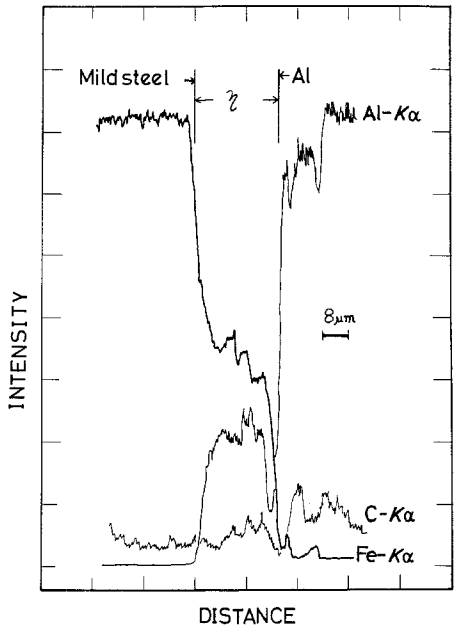

Figure 4 EPMA traces of Fe$K\alpha$, Al$K\alpha$ and C$K\alpha$ rays across the interface between mild steel and aluminium at an arc current of 130 A on a transfer-speed of 4.67 mm sec^{-1}.

(Fig. 8) [23], occurs on the aluminium side of the contact area with increasing iron concentration, whereas the formation of the intermetallic compound Fe_2Al_5 occurs on the iron side of the contact area, inherent in possessing the moderate concentration of aluminium in iron (Fig. 7c).

The crystallographic orientation of the intermetallic compounds such as Fe_2Al_5 and $FeAl_3$ appears to be dissimilar. In particular, there is considerably more anisotropy in the diffusion about the intermetallic compound Fe_2Al_5. That is, the η-phase is well known to have a preferential growth in the direction of the c-axis [6]. Therefore, it can be seen from the present experiment that the columnar Fe_2Al_5 intermetallic layer grows rapidly as tongue-like crystals perpendicular to bond plane (Fig. 7d). That is, it was thought that the η-phase layer develops in the heat-flux direction on solidification. As a result, it is noted that many vacancies result in the vicinity of the root of the Fe_2Al_5 layer, as can be seen in Fig. 3b. This vacancy phenomenon is probably due to Kirkendall effect [24, 25] and volume change of the intermetallic compound alloy layer on the rapid diffusion of the aluminium and the iron. A more detailed discussion of this respect may remain as a future problem.

5. Conclusions

The interfacial microstructures and intermetallic compounds produced by plasma arc butt fusion welding of aluminium to mild steel have been investigated. The principal results obtained from this analysis are summarized below.

1. The melt width in the bead weld and the alloy layer thickness of the intermetallic compound at the interfacial region decrease with the increasing transfer-speed of the plasma torch.

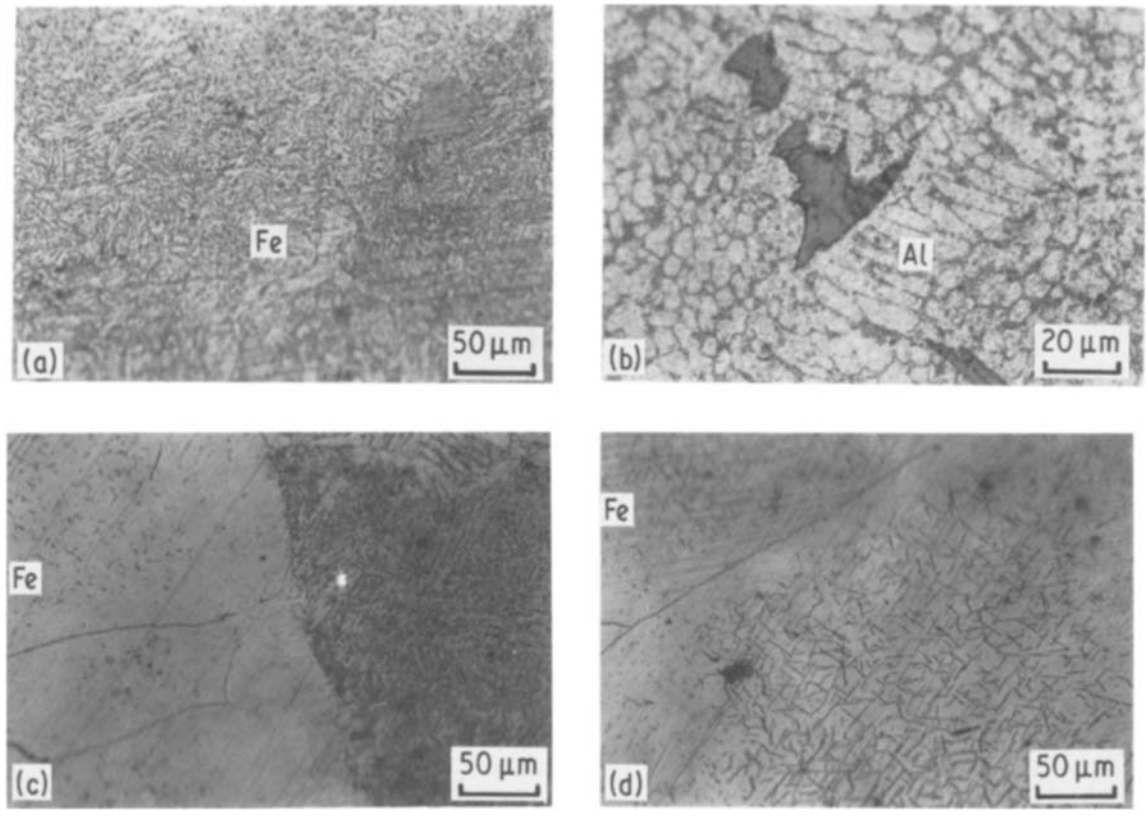

Figure 5 Microstructures of the melted zones of mild steel and aluminium, and the melted zone/unmelted zone interfacial regions. Nital etch. (a) Melted zone of mild steel refining the grain size. (b) Melted zone of aluminium having eutectic structure of β_2 and $FeAl_3$. (c) Fusion boundary region of the mild steel illustrating the formation of ferrite/minute pearlite interface. (d) Fusion boundary region of the mild steel exemplifying the ferrite/minute acicular pearlite interface.

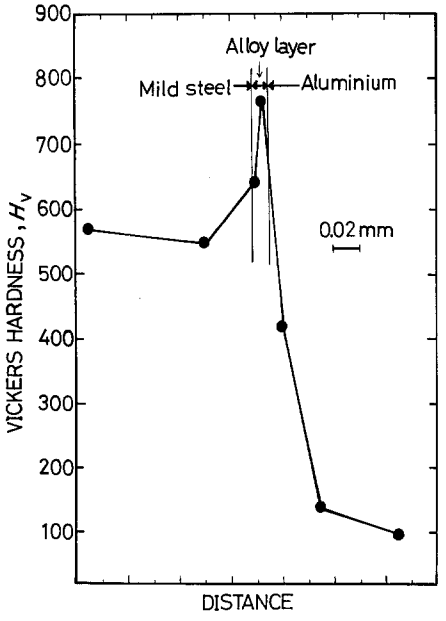

Figure 6 Vickers microhardness across the interfacial region between mild steel and aluminium, measured with a load of 50g.

2. The intermetallic layers formed at the interface between mild steel and aluminium are predominantly η-phase (Fe_2Al_5) and θ-phase ($FeAl_3$).

3. The columnar η-phase layer grows rapidly as tongue-like structure in the direction of the mild steel substrate and the granular θ-phase layer projects slowly to the aluminium during the course of solidification.

4. A porous structure can be visualized in the vicinity of the root of η-phase layer.

5. The structure of the melted zone and the fusion boundary of the mild steel change into grain refinement, whereas the melted zone of the aluminium has a eutectic structure of aluminium and θ-phase.

Acknowledgements

The author appreciates the financial support of the Japanese Ministry of Education for Scientific Research. In addition, the performance of EPMA work by Mr S. Oki is gratefully acknowledged.

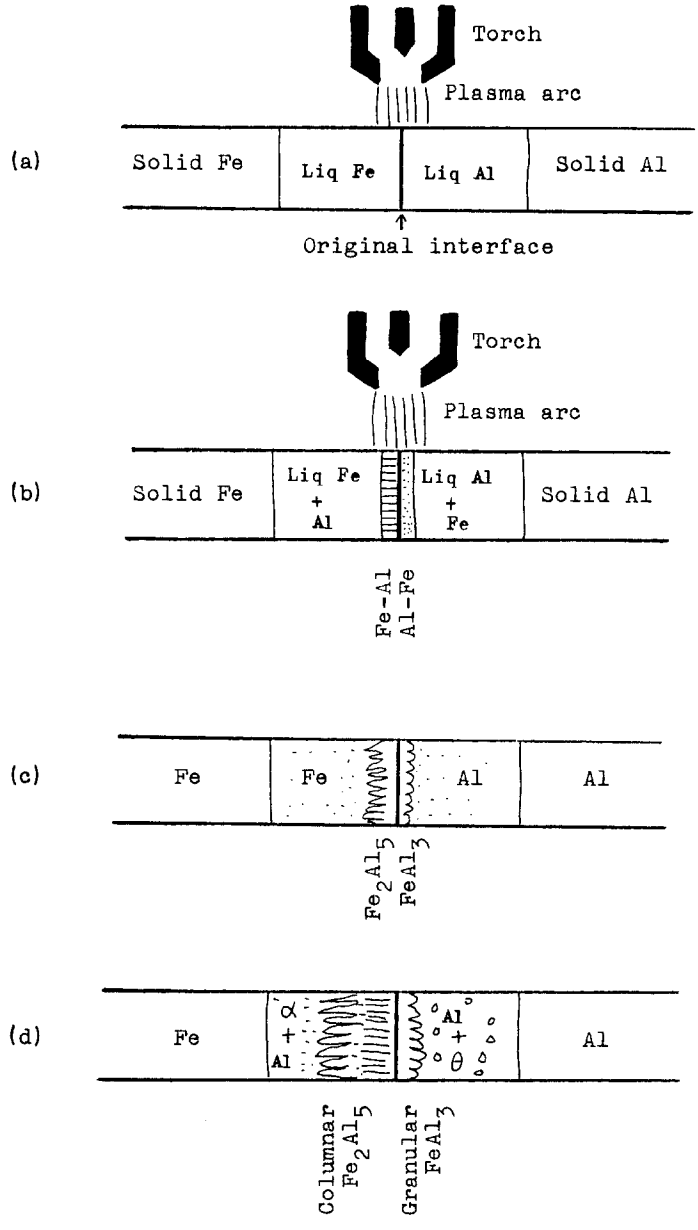

Figure 7 Schematic explanation of the plasma arc fusion welding of aluminium to mild steel and the alloy layer formation in the weld during solidification. (a) Contact reaction of molten mild steel with molten aluminium under the plasma arc heat source. (b) Mutual diffusion between the iron and the aluminium in the liquid state and the mutually saturated layer creations at the contact area. (c) Intermetallic compounds η (Fe_2Al_5)-phase and θ($FeAl_3$)-phase formations in the interfacial region immediately after solidification. (d) Rapid development of the η-phase and slow growth of the θ-phase in the interface region.

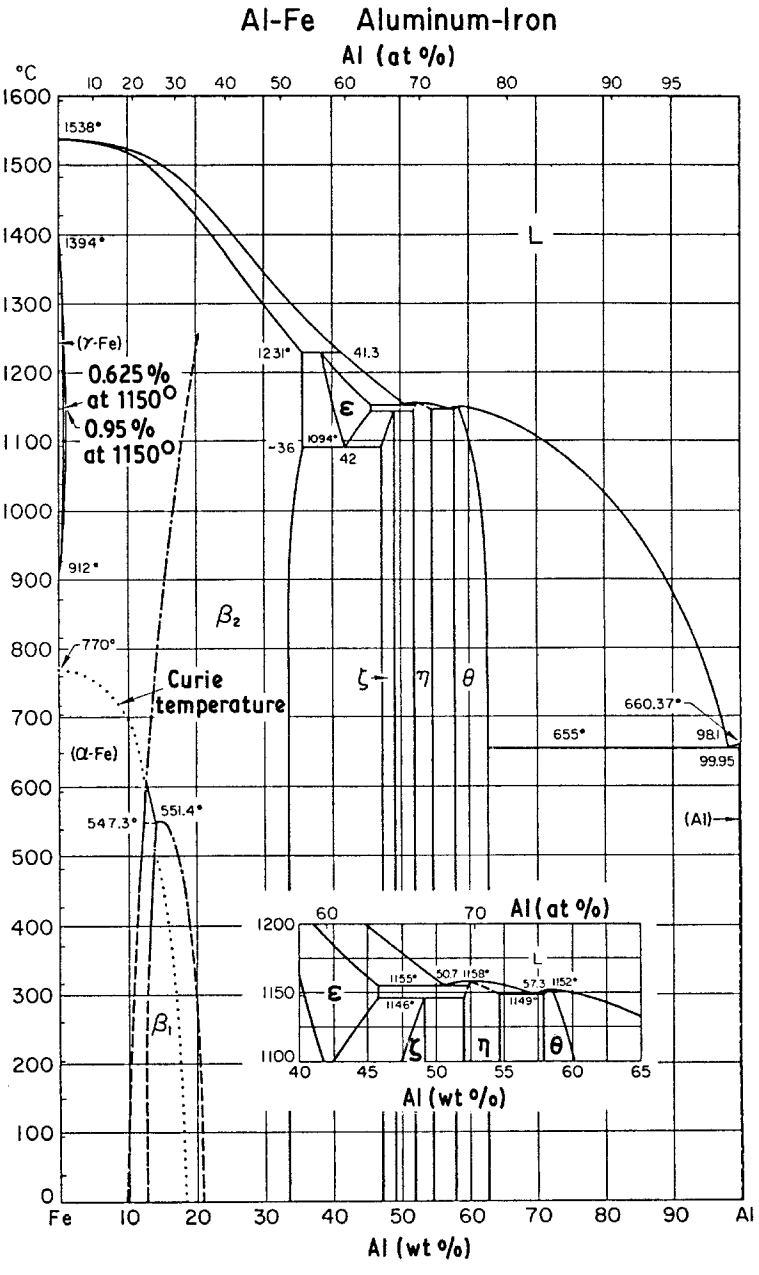

Figure 8 Al–Fe equilibrium diagram [23].

References

1. J. M. POPPLEWELL, T. G. CARRUTHERS and J. NUTTING, *J. Iron Steel Inst.* **105** (1967) 6.
2. I. N. ARCHANGELSKA and S. T. MILEIKO, *J. Mater. Sci.* **11** (1976) 356.
3. M. H. SCOTT and I. F. SQUIRES, *Brit. Weld. J.* **13** (1966) 151.
4. D. O. GITTINGS, D. H. POWLAND and J. O. MACK, *Tran. ASM* **43** (1951) 587.
5. Y. MITANI, R. VARGAS and M. ZAVALA, *Thin Solid Film* **111** (1984) 37.
6. T. HEUMANN and S. DITTRICH, *Z. Metalkde.* **50** (1959) 617.
7. V. N. YEREMENKO, YA. V. NATAZON and V. I. DYBKOV, *J. Mater. Sci.* **16** (1981) 1748.
8. M. NIINOMI, Y. EUDA and M. SANO, *Trans. Jpn Inst. Metal* **23** (1982) 780.
9. G. M. BEDFORD and J. BOUSTEAD, *J. Mater. Sci.* **13** (1978) 253.
10. E. R. NAIMON, J. H. DOYLE, C. R. RICE, D. VIGIL and D. R. WALMSLEY, *Weld. J.* **60** No. 11 (1981) 17.
11. S. K. MANNAN, V. SEETHARAMAN and V. S. RAGHUNATHAN, *Mat. Sci. Eng.* **60** (1983) 79.
12. M. A. MILLER and E. W. MASON, *Weld. J.* **35** (1956) 323s.
13. D. R. ANDREWS, *British Weld. J.* **9** (1962) 650.
14. G. MAH, P. S. MCLEOD and D. G. WILLIAMS, *J. Vac. Sci. Technol.* **11** (1974) 663.
15. H. SCHULTZ, *Schw.u.Schn.* **23** (1971) 421.
16. H. J. LAMB and M. J. WHEELER, *J. Inst. Metals* **92** (1963–1964) 150.
17. M. HANSEN and K. ANDERKO, "Constitution of Binary Alloys" 2nd edn. (McGraw-Hill, New York, 1958) p. 90.
18. K. NISHIDA and T. NARITA, *Trans. Jpn Inst. Metals* **14** (1973) 431.
19. S. KODA, S. MOROZUMI and A. KANAI, *J. Jpn Inst. Metals* **26** (1962) 764.
20. L. J. HÜTTER, H. STADELMAIER, A. C. FRAKER and R. G. HARDY, *Z. Metalkde.* **50** (1959) 625.
21. G. M. BEDFORD and J. B. BOUSTEAD, *Met. Technology* **1** (1974) 233.
22. Y. UEDA and M. NIINOMI, *Trans. Jpn Inst. Metals* **23** (1982) 709.
23. D. T. HAWKINS and R. HULTGREN, Metal Handbook 8th edn, Vol. 8, Metallography, Structures and Phase Diagrams (American Society of Metals, Ohio, 1973) p. 260.
24. R. E. REED-HILL, Physical Metallurgy Principles (D. Van Nostrand Co. Inc., London, 1984) p. 263.
25. Y. ADDA and J. PHILIBERT, *Acta Metall.* **18** (1960) 700.

Received 6 May
and accepted 23 July 1986